BIOMECHANICAL PILOT PROPERTIES IDENTIFICATION BY INVERSE KINEMATICS/INVERSE DYNAMICS MULTIBODY ANALYSIS

M. Mattaboni*, A. Fumagalli*, M. Jump, P. Masarati*, G. Quaranta***
***Politecnico di Milano, Dipartimento di Ingegneria Aerospaziale**
****Department of Engineering, The University of Liverpool**

Keywords: *Rotorcraft-Pilot Coupling, Biodynamics, Multibody System Dynamics*

Abstract

Pilot-vehicle interaction represents a critical aspect of aircraft design. In this work, experimental measurements of human body impedance, under realistic cockpit motion, are used to identify the direct transfer function between the motion of the seat and the controls inadvertently fed back into the rotorcraft, and the constitutive properties of the pilot's articulations. Only a reduced set of measurements is available, but the motion of the whole system can be reconstructed by means of inverse kinematics via kineto-static analysis in a multibody simulation framework, and the impedance of the articulations can be computed by direct parameter identification from the time histories of the reconstructed motion and the estimated forces. Preliminary applications to the aeroservoelastic simulation of rotorcraft are presented and discussed.

1 Rotorcraft-Pilot Coupling

Pilot-vehicle interaction represents a critical aspect of aircraft design, because it impacts performance, stability and safety in a manner that is only under the partial control of designers: the human factor. The history of aviation records a significant number of occurrences of critical pilot-vehicle interactions [1, 2]. These are often adverse and, in some cases, result in loss of aircraft and human lives.

This problem often appears in form of the so-called Pilot-Induced Oscillations (PIO) [3, 4]. Here, a sustained oscillatory motion of the aircraft is caused by an active, although unintended, intervention of the pilot on the aircraft's controls, in an attempt to counteract an adverse behavior, typically under the influence of misleading cues. When the destabilizing inputs are not the consequence of an active intervention of the pilot, but rather of a passive "impedance" interposed between the motion of the cockpit and the controls, the so-called Pilot-Augmented Oscillations (PAO) result.

Both occurrences are usually termed Aircraft-Pilot Couplings (APC) or, in the case of helicopters, Rotorcraft-Pilot Couplings (RPC). This terminology correctly shifts the emphasis from the pilot's contribution to that of the interface with the machine. In fact, despite being a subjective phenomenon, characterized by different proneness to instability for different pilots and different piloting attitudes, it is important to recognize the importance of the intrinsic proneness of the vehicle to unfavorable couplings.

While the aspects of the phenomenon directly related to an active participation of the pilot (PIO) have been extensively analyzed, primarily for fixed wing aircraft, only recently attention is being dedicated to the passive participation of the pilot (PAO) [5, 2], especially with respect to helicopters and rotorcraft.

Rotorcraft present a specific controls-related coupling issue, due to the presence of the col-

lective control. Traditionally, this device rotates about an axis parallel to the rotorcraft pitch axis, and is held by the pilot's left arm in a position that can range from nearly horizontal (minimum collective, arm almost fully extended) to some 45 degrees inclination (maximum collective, arm moderately bent). The collective control directly affects the rotor thrust; as such, a variation in thrust could accelerate the rotorcraft vertically, thus causing an unintentional change in collective input, that could cause further vertical imbalance.

Coupling between longitudinal and lateral cyclic controls and the corresponding rotorcraft horizontal motions appears less critical, since a change in cyclic does not usually cause an immediate horizontal force imbalance, but rather a pitch/roll rotation, which should be less prone to causing further action on the controls.

Tiltrotors could present similar types of coupling when flying in helicopter mode; in addition, roll could couple much more with lateral stick, since this control moment is commanded by differentially actuating the collective pitch of the two rotors.

All of the above described phenomena may be amplified by the deformability of the rotorcraft, both related to the aeroelasticity of the rotor and to the fuselage structural dynamics. This aeroservoelastic effect is twofold: first, it might enhance the amplitude of the coupling motion, and bring it into a frequency range slightly above the band-limited capabilities of the human body to effectively counteract it. Second, low-frequency phenomena may result in an intentional participation of the pilot with an amplitude that can impact the rotorcraft behavior, but with significant phase delays. This could potentially result in significant adverse responses.

2 Activity Description

The typical approach to RPC analysis consists in coupling the rotorcraft dynamics, $\boldsymbol{x}$, to the control inputs, $\boldsymbol{\delta}$, by adding a dynamic feedback model of the pilot in the form of either a transfer function, when operating in the frequency domain, or its state-space realization, when operating in the time domain, as indicated in Figure 1.

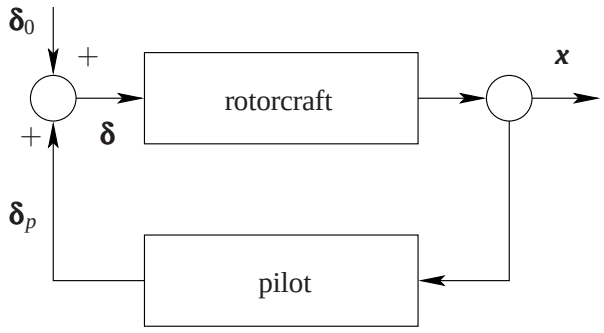

Fig. 1 Rotorcraft-Pilot Coupling (RPC) mechanical feedback loop.

A typical measure used to counteract adverse couplings consists in attenuating any adverse pilot's input, δ_p, by adding a notch filter between the control stick motion signal and the actual input that is fed into the Flight Control System (FCS).

This approach is consistent with current industrial practice, but suffers from a series of limitations, principally related to the fact that pilot transfer functions may present a marked variability, depending on parameters like:

- the size of the pilot (height and weight);
- the configuration of the pilot and the cockpit (what reference limb positions are considered);
- subjective piloting attitude;
- the task that is being performed (Mission Task Element, MTE);
- any additional workload the pilot is subjected to.

The variability related to the last three aspects cannot be eliminated or is not well understood yet. The variability related to the pilot's size cannot be eliminated either, although it can possibly be well predicted and taken into account. The variability related to the reference configuration is also well known, but cannot be easily handled with the previously illustrated approach, since it

requires that the impedance of the pilot be experimentally measured in all of the desired configurations, and possibly to interpolate between a discrete set of transfer functions when the required configuration is not exactly known.

The focus of the present activity is on the characterization of the pilot's biomechanics, for two purposes:

- to identify realistic biomechanical properties, to allow the detailed modeling of the pilot's impedance in a wide spectrum of sizes and postures, based on its deterministic modeling;

- to identify the effects of the pilot's task and workload on the biomechanical impedance.

The first objective has immediate practical applications: since it is known that the posture of the pilot, e.g. the average collective setting, has an impact on the corresponding impedance, the availability of a validated biomechanical model would allow linearized transfer functions to be extracted directly from the nonlinear multibody model, without the need to resort to identifying experimental measures.

The second objective aims to understand if and how the task and the workload impact upon the pilot's impedance, in order to be able to determine the worst-case characteristics to be used in subsequent aeroservoelastic analyses. It is also hoped that it will shed some further light on the correlation between the operational and dynamic aspects of man-machine interaction. This latter aspect will not be addressed in the present paper, since no related experimental activity has been performed yet.

So far, a biomechanical experimental campaign has been performed using the Bibby flight simulator at the University of Liverpool (UOL). More testing will take place in the near future at Liverpool, while a dedicated biomechanical testing facility will be set up at Politecnico di Milano (POLIMI).

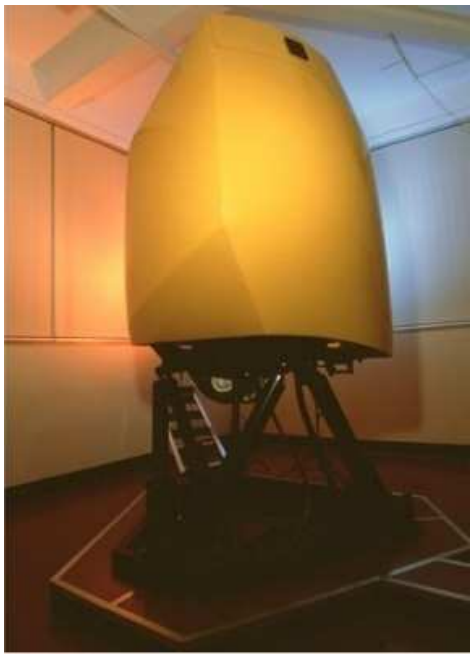

Fig. 2 Bibby Flight Simulator

3 Experimental Set-Up

The testing was conducted at The University of Liverpool's (UOL) Flight Science and Technology (FST) Research Group's Bibby flight simulation laboratory. The primary research tool available to FST is a six visual channel flight simulator mounted upon a six-axis motion base, Figure 2. This facility is described in its original form in Ref. [6]. The primary modelling tool used to generate research vehicle model's is Advanced Rotorcraft Technologies' (ART) FLIGHTLAB software (Ref. [7]). This interfaces with ART's PILOTSTATION software to provide the motion cueing to the simulator pilot. The usual use to which the simulator is put requires the development of an air-vehicle model of the desired fidelity. However, the operation of that model, including the use of motion cueing and the subsequent recording of test data is all handled automatically by the facility hardware and software. The proposed experimentation required that new capabilities be developed (or procured) to achieve the test objectives, viz:

1. develop a method to drive the existing motion system without reference to a specific

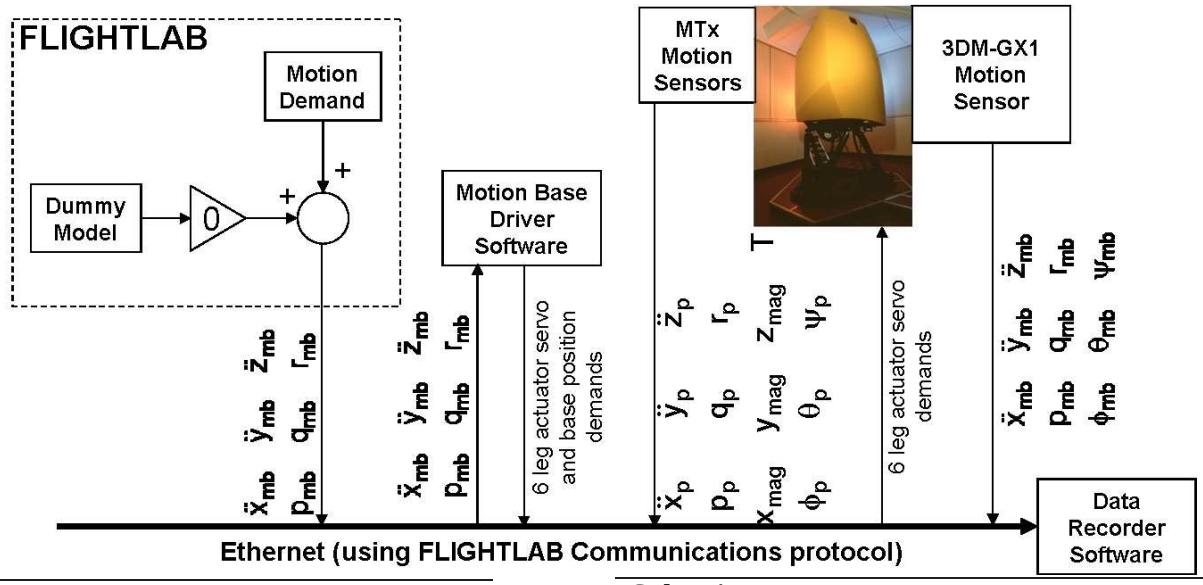

Notation

x	x measurement axis of motion sensor
y	y measurement axis of motion sensor
z	z measurement axis of motion sensor
p	roll rate
q	pitch rate
r	yaw rate
ϕ	roll angle
θ	pitch angle
ψ	yaw angle
T	temperature

Subscripts

mb	of the simulator motion base
p	of the pilot/simulator occupant
mag	magnetic field

Glossary

FST	Flight Science and Technology research group
UOL	University of Liverpool
POLIMI	Politecnico di Milano

Fig. 3 Schematic diagram of experimental set-up.

vehicle model;

2. measure the input demands to the motion system;

3. measure the angles, rates and accelerations of the simulator pod (i.e. the motion stimulus to the simulator occupant);

4. measure the resultant pilot's arm motion, and

5. capture all of the experimental data from the various sources of measurement.

Figure 3 shows schematically how these objectives were achieved. To achieve capability 1, a dummy FLIGHTLAB model was created whose motion-demand outputs were all set to zero. The desired input to the motion base was then injected via the simulation model's control system, the output of which was directed to the six motion system data latches that are the 'input' to the motion base control software. To achieve the second capability requirement, a new version of the motion-base controller software was created to broadcast the inputs and outputs of the latch filters. To measure the motion of the motion-base itself, a MicroStrain 3DM-GX1 motion sensor was procured by UOL and to measure the pilot arm motion, two Xsens MTx sensors were purchased by POLIMI. For all of these sensors, software had to be developed to broadcast the data that they were measuring. Finally, a set of software had to be developed to capture and save all of the data being broadcast across the simulation

Table 1 Independent experimental variables.

Independent Variable	Values
Excitation axis	Heave (up-down); Surge (fore-aft)
Excitation amplitude	0.1g; 0.2g
Excitation type	Sinusoidal frequency sweep (stepped); random
Collective nominal start position	10%; 50%; 90%

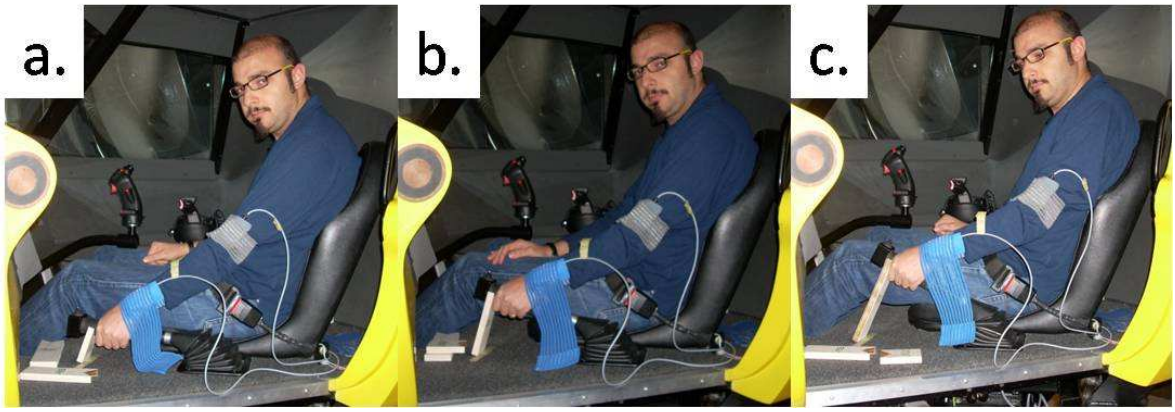

Fig. 4 Nominal collective lever start positions: (a) 10%; (b) 50% and (c) 90% of full scale deflection.

facility Ethernet.

3.1 Test Procedure

With the hardware and software configured as described above, the human subject was seated in the simulator cockpit and the MTx motion sensors attached near to the wrist and the elbow. A typical arrangement is shown in Figure 4(a). The controls (longitudinal and lateral cyclic stick, collective lever, rudder pedals) were set to their nominal start positions, the occupant locked into the pod and the motion platform raised. The excitation for the current test point was applied and the results recorded for later analysis. Table 1 shows the independent variables used for the experimentation. Figure 4 shows the three nominal collective positions noted in Table 1. Figure 5 shows an example of the first part of one of the heave axis excitation demands applied to the motion base. It is a sinusoidal frequency sweep starting at 0.4Hz that steps up in 0.2Hz increments to the final value of 7.0Hz (not shown in the Figure).

The majority of the test points required that the collective lever forces be switched off. The

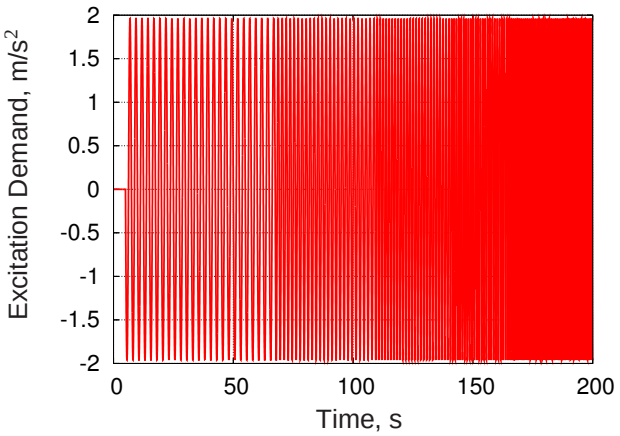

Fig. 5 Example excitation demand profiles for the heave axis.

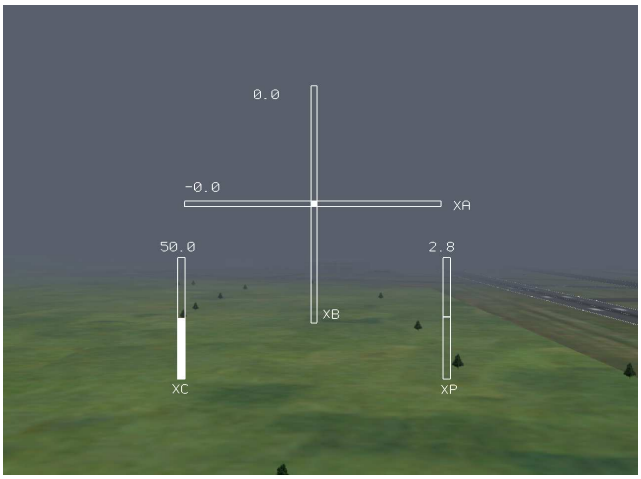

Fig. 6 Control inceptor position display.

ideal situation was one of zero friction. In practice, this was not possible with the simulator hardware and the best that could be achieved was that the collective lever forces were set to the minimum available. This initially presented an issue in that, with the stick forces switched off, the collective became 'floppy' and had to be physically held in the desired start positions. However, it was important that any collective and hence arm vibration were restricted to be approximately around this nominal start position during a given test. To assist with this task, a pilot display was created as shown in Figure 6. The display provided the simulator occupant and operators with an indication of all of the control inceptor positions. The left-most symbol shows collective lever position, the central cross-shaped symbol shows longitudinal and lateral cyclic position and the right-most symbol shows rudder pedal position. If the subject's arm response to the applied excitation was such that the stick position deviated by more than 10% of full-scale deflection from the nominal start position, then the occupant was instructed to return the collective lever to that position using the display as a guide.

3.2 Raw Results Data

Figure 7 presents an example, for a 0.2g heave test case, of some of the key data items recorded during the test campaign. These are the excitation applied to the motion base platform measured by the 3DM-GX1 motion sensor (Figure 7(a)), the measured collective stick position (Figure 7(b)), the demanded motion base heave position (Figure 7(c)) and the resultant motion at the pilot wrist measured using one of the MTx units (Figure 7(d)). These data then formed the basis for the subsequent analysis to generate a transfer function and multibody bio-mechanical pilot model.

4 Transfer Function Identification

A common approach to the modeling of the pilot's influence on aeroservoelasticity consists in identifying an equivalent transfer function that relates the motion of the controls in response to the vibratory load the pilot receives from the seat. Single Input-Single Output (SISO) models are often used. This approach may be questionable from many points of view, as the effects of different sources of vibration may not be easily separated. However, it provides a simple and useful tool to consider the problem to a first approximation.

In the literature there are quite a few examples of experimental transfer functions identified for similar purposes. In many cases, they address the very low frequency range that is typical of flight mechanics of fixed wing aircraft.

An example of transfer functions specifically intended for rotorcraft analysis are provided by Mayo in [8] for the collective control, and by Parham *et al.* in [9] for the V–22 longitudinal cyclic control. In this paper, the focus is on the collective control.

In [8], two functions are proposed, for pilots of different size. These are called 'ectomorphic' (smaller size) and 'mesomorphic' (larger size). Here only the mesomorphic function,

$$H_{\text{meso}} = \frac{4.02s + 555.4}{s^2 + 13.31s + 555.4}, \qquad (1)$$

is considered, since in [10] it appeared to be the most prone to instability when coupled to a light helicopter. In the original reference, [8], the ectomorphic function appeared to be more prone to

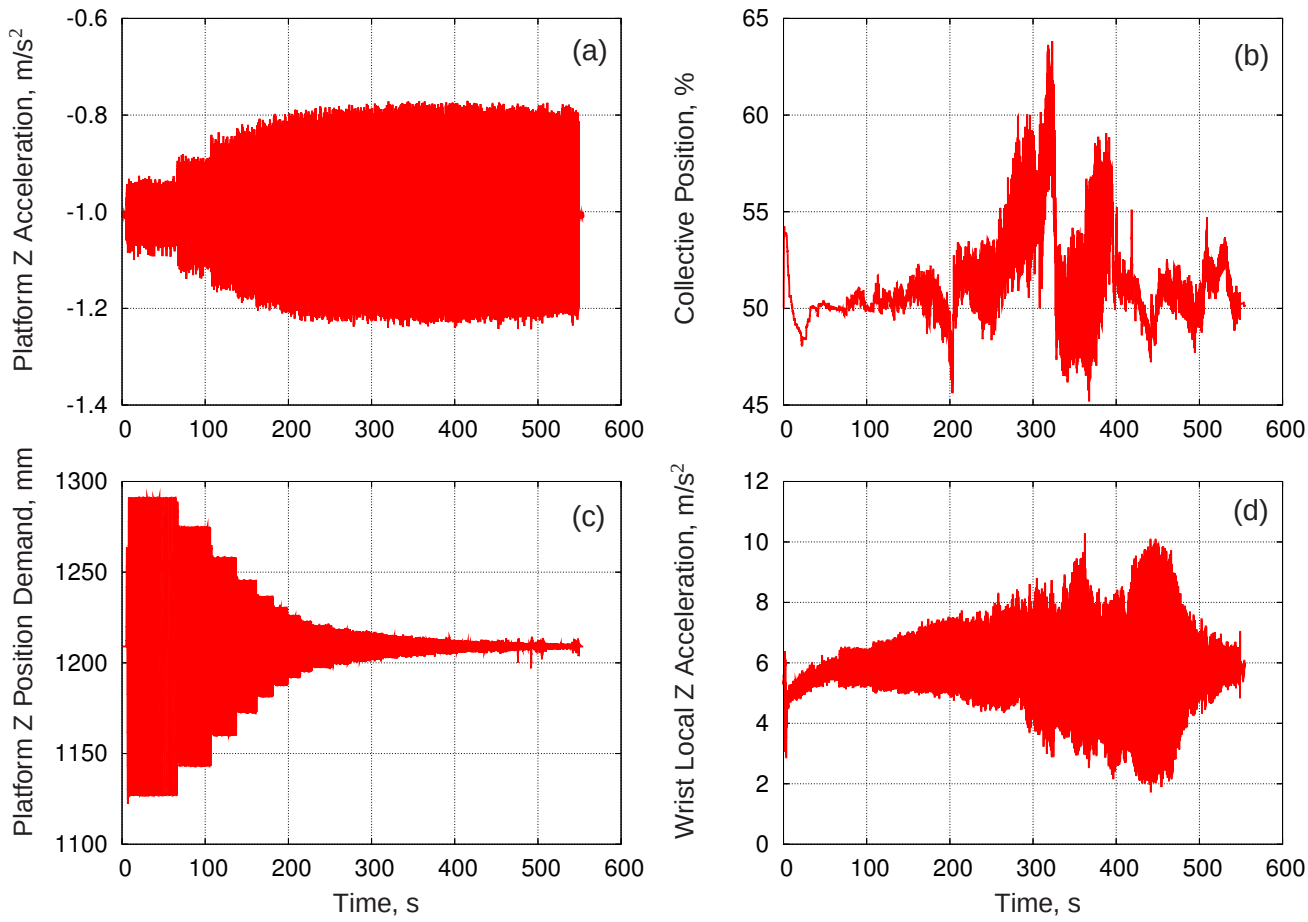

Fig. 7 Selected recorded outputs for a 0.2g heave excitation test case: (a) measured platform heave acceleration; (b) collective lever position; (c) platform heave position demand; and (d) local heave acceleration for the subject's wrist.

instability when coupled with the dynamics of a heavy helicopter.

The transfer function of Eq. (1) represents the absolute acceleration of the hand holding the collective control stick as a function of the vertical acceleration of the seat. In order to apply it to a multibody analysis code in the time domain, it has been modified to return the relative motion of the stick by adding a double pseudo-integrator,

$$H'_{\text{meso rel}} = \frac{1}{s}\frac{1}{s+\alpha}\left(H_{\text{meso}} - 1\right), \qquad (2)$$

where the first integrator $1/s$ cancels the zero in the origin resulting from the $H(s)-1$ term, while the second has been arbitrarily modified into $1/(s+\alpha)$, with α corresponding to a very low frequency pole (0.1 Hz in the present case) to eliminate any possible drift. The rationale is that at very low frequencies, the pilot can compensate any acceleration that causes arm movement, so a static acceleration can result at most in static deflection of the control. In any case, the very low frequency behavior of the pilot is outside the scope of the present work.

The amplitude and phase of the function of Eq. (2) is compared in Figure 8 to those obtained by identifying the motion of the collective control stick held by a pilot, measured in the flight simulator in response to a vertical acceleration imposed by the base. The measured output of the experiment, namely the % rotation of the collective control stick, has been transformed into the displacement orthogonal to the stick at the han-

dle, in order to make it comparable with the function of Eq. (2). The resulting functions seem to be characterized by a 4th order denominator and a 2nd order numerator, respectively made by two pairs of complex conjugated poles and one pair of complex conjugated zeros, namely

$$H' = G\frac{(s-z)(s-z^*)}{(s-p_1)(s-p_1^*)(s-p_2)(s-p_2^*)}, \quad (3)$$

where G is the gain (in % of collective as a function of the seat acceleration in m/s^2), z is the zero and p_1, p_2 are the poles; the identified values are reported in Table 2. This function is structurally different from that of Eq. (2), which has a 3rd order denominator and a 1st order numerator. The pilot's behavior described by the identified function appears to be characterized by two frequencies, the lower similar to that in [8].

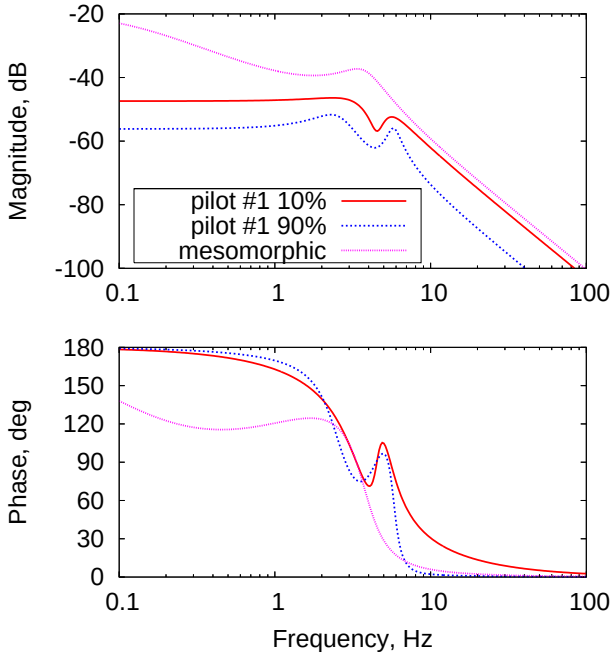

Fig. 8 Pilot transfer functions frequency response.

Figure 8 compares Ref. [8]'s mesomorphic pilot to pilot #1 at 10% and 90% reference collective control stick position.

It is worth noticing that, according to Figure 9, there are two dominant frequencies in the pilot's response to a random vertical shaking of the cockpit, corresponding to the two pilot's

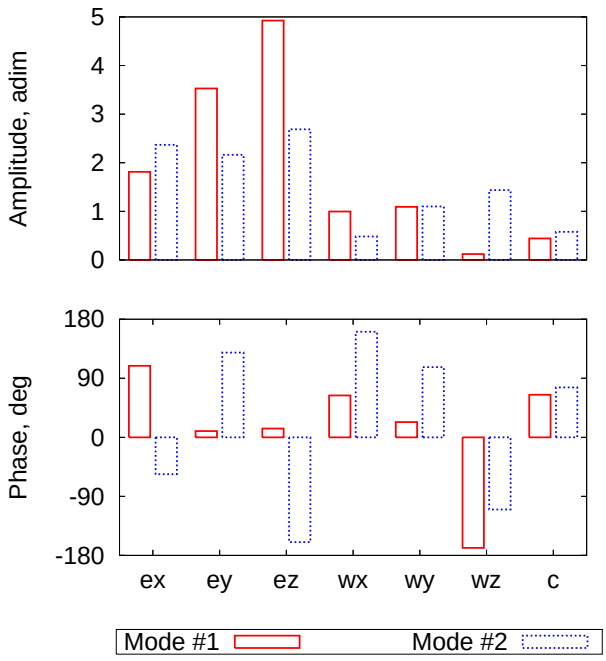

Fig. 9 Accelerations relative to the flight simulator base and % collective control stick rotation for random base acceleration input.

poles in Table 2. The Figure shows the results of the Proper Orthogonal Decomposition (POD) of the accelerometer measurements taken at the elbow ('ex', 'ey', 'ez') and at the wrist ('wx', 'wy', 'wz'), and of the collective control stick rotation ('c', in %/(m/s^2)), normalized by the corresponding base acceleration input. The acceleration components are relative to the flight simulator base, projected in the Earth reference frame.

The sensor located close to the elbow shows a much larger response than the one close to the wrist. The motion of the sensor close to the wrist, which is closely related to the motion of the collective control stick handle, appears to be dominated by a motion in direction x (fore-aft) for mode #1, and by a motion in direction z (vertical) for mode #2. On the contrary, the motion of the elbow is dominated by its vertical component for mode #1, while all components show a similar participation for mode #2. Both sensors show a noticeable participation of lateral motion for both modes.

The phase clearly shows that the modes are

Table 2 Identified transfer functions properties, % collective for seat acceleration in m/s^2, Eq. (3).

Test	Pole #1	Pole #2	Zero	Gain
Pilot #1, 10%	-9.8189 ± 20.4374i	-7.0661 ± 31.2961i	-2.6282 ± 28.3482i	-4465.3
Pilot #1, 50%	-6.6574 ± 19.3086i	-4.9026 ± 35.8785i	-3.5630 ± 27.6716i	-2446.1
Pilot #1, 90%	-4.6876 ± 15.3775i	-3.5824 ± 36.1740i	-7.3902 ± 27.8659i	-1024.9
Pilot #2, 10%	-12.2048 ± 19.8534i	-5.0502 ± 33.7910i	-3.2423 ± 30.9463i	-4431.7
Pilot #2, 50%	-5.9031 ± 16.9689i	-7.7169 ± 38.3072i	-5.7946 ± 24.1660i	-2322.5
Pilot #2, 90%	-1.9331 ± 12.6278i	-6.1569 ± 37.2060i	-6.5938 ± 18.3922i	-1189.0

definitely complex; it is worth noticing that, as expected, the % collective control stick rotation is almost directly out of phase with respect to the acceleration of the wrist.

5 Multibody Biomechanics Modeling

The topic of analyzing and simulating the behavior of biological systems, including the human body, has been widely addressed by means of multibody techniques [11, 12, 13, 14, 15]. Many authors focused on identifying model parameters from experiment [16]. Specific attention to the biodynamic modeling of pilots for the purpose of analyzing their interaction with the flight dynamics of fixed wing aircraft has been paid by some authors, significantly in the area of roll-ratcheting [17].

In this work, a general-purpose multibody simulation analysis, based on the free software MBDyn [18], typically used for (but not limited to) rotorcraft aeroservoelasticity, has been applied to the identification of the constitutive behavior of the pilot's articulations. A sketch of the partial pilot biomechanical model is shown in Figure 10. This presents the arm of the pilot in the three configurations measured during the tests. The objective of the analysis consists in estimating the constitutive properties of the pilot's articulations, based on a statistical estimate of the corresponding limbs' inertia properties, and on (partial) kinematics (and force) measurements of the pilot during appropriate shake test sessions.

In many cases available from the literature, the level of detail of the biomechanical models entails the modeling of each muscle, with specific aspects of muscle actuation, applied on top of a detailed model of the musculo-skeletal system [11]. However, in the present work, the interest is rather on modeling a mechanical equivalent of the human body, capable of reproducing the body's dynamic behavior for relatively small oscillations about kinematically consistent configurations, so a more coarse level of biomechanical modeling has been considered.

5.1 Motion Estimate from Kineto-Static Analysis

The first step consists in performing a kineto-static analysis of the biomechanical model, to estimate the motion of the entire model based on the available kinematic measurements, by inverse kinematics.

As illustrated in [19], general-purpose multibody dynamics analysis can be used to solve the kinematic inversion of arbitrarily complex systems subjected to kinematic constraints. In the present case, a system of b independent rigid bodies, representing the limbs of the human body, is constrained by a kinematic relationships that describe the articulations. Typically, $b = 17$, while the constraints, accounting for 14 mixed spherical and revolute articulations, allow a significant number of degrees of freedom. For example, the elbow and the knee are represented by revolute joints, while the shoulder and the wrist are modeled as spherical joints. The motion of the limbs is described by Lagrangian coordinates $\boldsymbol{q}$ that directly consist in the position and orientation of

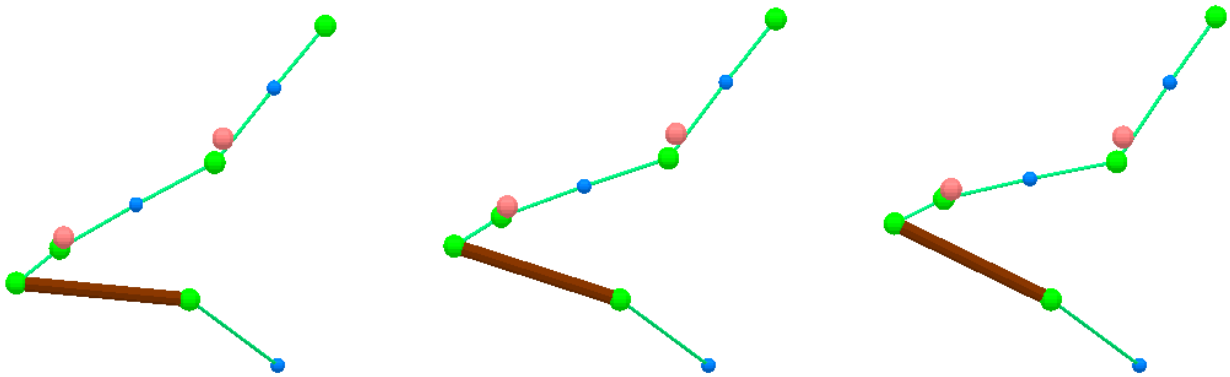

Fig. 10 Multibody model of the pilot's arm holding the collective control stick at 10, 50 and 90%. The MTx sensors are located close to the elbow and close to the wrist.

some reference point on the limbs, $\boldsymbol{x}_i$ and $\boldsymbol{R}_i$. The scleronomic constraints that model the articulations are algebraic relationships that relate the coordinates $\boldsymbol{q}$, namely

$$\boldsymbol{\Phi}(\boldsymbol{q}) = \mathbf{0}, \tag{4}$$

leaving only a minimal number of degrees of freedom, corresponding to those allowed by the articulations.

When kinematic inversion is addressed, the kinematics of the whole system need to be determined, either because imposed, or because restrained by the system's algebraic constraints. The imposition of the motion of some limbs, e.g. of the hands when grabbing the controls, is described by an additional set of d rheonomic constraints, namely

$$\boldsymbol{\Psi}^*(\boldsymbol{q}, t) = \mathbf{0}, \tag{5}$$

usually in the form

$$\boldsymbol{\Psi}(\boldsymbol{q}) = \boldsymbol{\theta}(t). \tag{6}$$

This relationship, coupled to that of Eq. (4), cannot usually be inverted analytically, to express the motion of a generic system as a function of the drivers $\boldsymbol{\theta}(t)$.

Moreover, during the execution of typical environment interaction tasks, the human body represents an under-determined system, since its articulations allow multiple configurations for specific imposed motion of hands, feet and torso (since pilots usually sit in the cockpit).

As a consequence, there will exist $f = 6 \cdot b - a - d$ degrees of freedom that need to be determined to correctly analyze the human body's behavior. The problem can be addressed in different manners. Typically, the motion of as many limbs as possible is measured, usually by optical techniques. However, in the present case, the need to operate within the enclosed cockpit of the flight simulator prevented this opportunity; in any case, optical motion acquisition is not considered a viable option for vibration analysis.

The problem was addressed by acquiring limb motion information by means of integrated inertial devices, namely the previously mentioned Xsens MTx, providing 3-axis accelerometer and gyro measurements. The devices were applied to the arm and the forearm of interest, thus limiting the analysis to a simple loop consisting of the torso and the left arm of the pilot (the one holding the collective control).

The missing motion states can be recovered according to the procedure detailed in [19] by restraining the remaining degrees of freedom with arbitrary springs while performing a purely kinematic analysis, namely

$$\boldsymbol{K}\boldsymbol{q} + \boldsymbol{\Phi}_{/\boldsymbol{q}}^T \boldsymbol{\lambda} + \boldsymbol{\Psi}_{/\boldsymbol{q}}^T \boldsymbol{\mu} = \mathbf{0} \tag{7a}$$

$$\boldsymbol{\Phi}(\boldsymbol{q}) = \mathbf{0} \tag{7b}$$

$$\boldsymbol{\Psi}(\boldsymbol{q}) = \boldsymbol{\theta}(t), \tag{7c}$$

whose linearization

$$\begin{bmatrix} \boldsymbol{K} & \boldsymbol{\Phi}_{/\boldsymbol{q}}^T & \boldsymbol{\Psi}_{/\boldsymbol{q}}^T \\ \boldsymbol{\Phi}_{/\boldsymbol{q}} & \boldsymbol{0} & \boldsymbol{0} \\ \boldsymbol{\Psi}_{/\boldsymbol{q}} & \boldsymbol{0} & \boldsymbol{0} \end{bmatrix} \begin{Bmatrix} \Delta\boldsymbol{q} \\ \Delta\boldsymbol{\lambda} \\ \Delta\boldsymbol{\mu} \end{Bmatrix} = -\begin{Bmatrix} \boldsymbol{K}\boldsymbol{q}+\boldsymbol{\Phi}_{/\boldsymbol{q}}^T\boldsymbol{\lambda}+\boldsymbol{\Psi}_{/\boldsymbol{q}}^T\boldsymbol{\mu} \\ \boldsymbol{\Phi}(\boldsymbol{q}) \\ \boldsymbol{\Psi}(\boldsymbol{q}) \end{Bmatrix} + \begin{Bmatrix} \boldsymbol{0} \\ \boldsymbol{0} \\ \boldsymbol{\theta}(t) \end{Bmatrix} \quad (8)$$

is equivalent to the Moore-Penrose pseudo-inverse if an isotropic stiffness matrix

$$\boldsymbol{K} = k\boldsymbol{I} \quad (9)$$

is used. Otherwise, by tailoring the relative stiffnesses, the solution can be shaped nearly at will.

By adding dead loads to the right-hand side of Eq. (7a), the solution can be shaped further; a typical application consists of adding gravity to cause the pilot's arm to assume a configuration with its center of gravity as close as possible to the lowest position, which naturally resembles the pilot at rest.

5.2 Articulation Forces from Inverse Dynamics

An inverse dynamics analysis [20] can be used to estimate the internal forces and moments in the articulations, which are subsequently used, along with the imposed relative motion, to identify the corresponding mechanical impedance.

However, this analysis requires the biomechanical model to have a tree-like topology, which is not the case of a pilot sitting in the cockpit and holding the controls, unless reaction forces and moments are measured at some location (e.g. within the controls); unfortunately, this was not possible. This problem can be partially circumvented by resorting to a power balance.

Consider a dynamic system made of rigid bodies whose zero, first and second-order inertia moments are m_i, $\boldsymbol{S}_i$, $\boldsymbol{J}_i$, and of generic 3D and, occasionally, 6D lumped deformable components whose constitutive properties are expressed as functions of the relative strain and strain rate.

The inertia of the human body parts is estimated based on age, gender, height and weight of the pilot, according to the GEBOD database [21].

For simplicity, only elastic and viscoelastic components are considered, so that the value of the corresponding forces and moments only depends on the instantaneous value of the relative strain and strain rate, namely

$$\boldsymbol{f}_i = \boldsymbol{f}_i\left(\boldsymbol{d}_i, \dot{\boldsymbol{d}}_i\right) \quad (10)$$

and

$$\boldsymbol{m}_i = \boldsymbol{m}_i\left(\boldsymbol{\theta}_i, \dot{\boldsymbol{\theta}}_i\right) \quad (11)$$

for linear and angular strain components, respectively, where $\boldsymbol{d}$ and $\boldsymbol{\theta}$ are the linear and angular strains. In most cases, a linear viscoelastic constitutive law will be actually considered in the present work, but the procedure applies to more general cases.

As the system is only subjected to an external excitation coming from the motion of the base, the power introduced by moving the base must be turned into either kinetic or potential energy, or dissipated by the deformable components that model the articulations:

$$\frac{\mathrm{d}}{\mathrm{d}t}E_c = \Pi_{\text{base}} + \Pi_{\text{gravity}} + \Pi_{\text{articulations}}, \quad (12)$$

with

$$\Pi_{\text{base}} = \dot{\boldsymbol{x}}_{\text{base}} \cdot \boldsymbol{f}_{\text{base}} \quad (13a)$$

$$\Pi_{\text{gravity}} = \sum_i \dot{\boldsymbol{x}}_i m_i \cdot \boldsymbol{g} \quad (13b)$$

$$\Pi_{\text{articulations}} = -\sum_j \dot{\boldsymbol{\theta}}_j \cdot \boldsymbol{m}_j\left(\boldsymbol{\theta}_j, \dot{\boldsymbol{\theta}}_j\right). \quad (13c)$$

where the power introduced by the motion of the base, Eq. (13a), is not known, as well as that involved in straining the articulations, Eq. (13c).

However, knowledge of the motion of the whole system allows the inverse dynamics problem of the system to be solved after arbitrarily opening the chain, by disconnecting the collective control stick, in order to avoid any indetermination in the internal forces:

$$\frac{\mathrm{d}}{\mathrm{d}t}E_c = \Pi'_{\text{base}} + \Pi_{\text{gravity}} + \Pi'_{\text{articulations}}, \quad (14)$$

with

$$\Pi'_{\text{base}} = \dot{\boldsymbol{x}}_{\text{base}} \cdot \boldsymbol{f}'_{\text{base}} \quad (15a)$$

$$\Pi'_{\text{articulations}} = -\sum_j \dot{\boldsymbol{\theta}}_j \cdot \boldsymbol{m}'_j; \quad (15b)$$

$\boldsymbol{m}_j$ are the couples computed by the inverse dynamics to impose the desired motion to the articulations. Disconnecting the collective control stick does not alter the power involved, since during the tests minimal friction (although not zero) nor other source of torque resisted its motion.

The resulting articulation couples $\boldsymbol{m}_j$ will differ from the real ones, since the topology of the system was modified by removing the collective control stick. However, the corresponding overall power must be equal to that involved in straining the deformable articulations. As a consequence, the relationship

$$\Pi_{\text{articulations}} = \Pi'_{\text{articulations}} - \left(\Pi_{\text{base}} - \Pi'_{\text{base}}\right) \tag{16}$$

can be written for each sampling time. There is no guarantee that the term $\left(\Pi_{\text{base}} - \Pi'_{\text{base}}\right)$ vanishes, but the error appears to remain limited. The power balance at each time step allows to estimate the parameters of the constitutive law of the joints in a least-squares sense.

So far, this approach showed an appreciable capability to recover the stiffness properties of a model representing the pilot's arm from the results of a direct simulation. However, its application to the results of the previously described experiments was not successful enough. In fact, in some cases, definitely unreliable stiffness properties of the articulations have been obtained: for example, non-positive definite stiffness matrices, when looking for linear viscoelastic constitutive properties, have been obtained. Nonetheless, this approach appears very promising, and thus will be pursued further in future work.

5.3 Direct Least-Squares Parameter Estimate

As an alternative to the previous approach, the direct determination of the constitutive model of the articulations can be performed without resorting to inverse dynamics, by exploiting the Virtual Power Principle (VPP).

The parameter identification requires the virtual power associated with all forces and moments, except those related to articulations, to be known. This, in turn, requires the knowledge of the kinematics related to motion-dependent forces and moments, and of the corresponding virtual velocities. An estimate of the kinematics related to motion-dependent forces and moments can be easily obtained from the initial kineto-static analysis.

The corresponding virtual velocities can be obtained from the same analysis after some manipulation. By definition, the virtual velocities must be admissible, which means that they must be compatible with the constraints at fixed time. As soon as the system is supposed to be made of ideal constraints, including those that are used to impose its motion, the constraints themselves do not contribute any virtual power to the system. As such, an instance of the virtual velocities can be obtained from the actual velocities of the system, after subtracting any velocity related to the motion of the constraints; in other words, assuming a relationship

$$\boldsymbol{x} = \boldsymbol{x}(\boldsymbol{q}, t) \tag{17}$$

between the Lagrangian coordinates $\boldsymbol{q}$ and the motion $\boldsymbol{x}$ of a portion of the system, the velocity is

$$\dot{\boldsymbol{x}} = \boldsymbol{x}_{/\boldsymbol{q}}\dot{\boldsymbol{q}} + \boldsymbol{x}_{/t}, \tag{18}$$

while the virtual velocity is

$$\delta\dot{\boldsymbol{x}} = \boldsymbol{x}_{/\boldsymbol{q}}\delta\dot{\boldsymbol{q}}. \tag{19}$$

So, among all the admissible ones, a value of $\delta\dot{\boldsymbol{x}}$ that satisfies its requirements can be recovered from the actual velocity $\dot{\boldsymbol{x}}$ by computing

$$\delta\dot{\boldsymbol{x}} = \dot{\boldsymbol{x}} - \boldsymbol{x}_{/t}. \tag{20}$$

The virtual power associated with the inertia and gravity forces is

$$\begin{aligned}\delta\mathcal{P}_{\text{inertia}_i} = \\ -\delta\dot{\boldsymbol{x}}_i\left(m_i\left(\ddot{\boldsymbol{x}}_i + \boldsymbol{g}\right) + \dot{\boldsymbol{\omega}}_i \times \boldsymbol{S}_i + \boldsymbol{\omega}_i \times \boldsymbol{\omega}_i \times \boldsymbol{S}_i\right) \\ -\delta\boldsymbol{\omega}_i\left(\boldsymbol{S}_i \times \left(\ddot{\boldsymbol{x}}_i + \boldsymbol{g}\right) + \boldsymbol{J}_i\dot{\boldsymbol{\omega}}_i + \boldsymbol{\omega}_i \times \boldsymbol{J}_i\boldsymbol{\omega}_i\right).\end{aligned} \tag{21}$$

The virtual power associated with a generic linear and angular deformable component is

$$\begin{aligned}\delta\mathcal{P}_{\text{articulations}_j} = \\ -\delta\dot{\boldsymbol{d}}_j\boldsymbol{f}_j\left(\boldsymbol{d}_j, \dot{\boldsymbol{d}}_j\right) - \delta\dot{\boldsymbol{\theta}}_j\boldsymbol{m}_j\left(\boldsymbol{\theta}_j, \dot{\boldsymbol{\theta}}_j\right).\end{aligned} \tag{22}$$

In the analysis of the biomechanical behavior of an articulation, two essential factors can come into play:

- the change in the reference elongation of the muscles; this is based on voluntary attention of the pilot;
- the relaxation of the muscle due to fatigue, which is related to the load it is carrying.

The first factor can be quite important especially when the pilot is performing some specific task. In this case, the strain that enters the constitutive law,

$$\boldsymbol{\theta} = \boldsymbol{\theta}_{\mathrm{el}} + \boldsymbol{\theta}_{\mathrm{c}}, \tag{23}$$

must be seen as made of an 'elastic' fraction, $\boldsymbol{\theta}_{\mathrm{el}}$, and of an 'inelastic' fraction, $\boldsymbol{\theta}_{\mathrm{c}}$, which corresponds to the change in the neutral reference motion that is commanded by the pilot's attention. The latter fraction does not participate in the virtual velocity:

$$\delta\dot{\boldsymbol{\theta}} = \delta\dot{\boldsymbol{\theta}}_{\mathrm{el}} \tag{24}$$

In the present work, this factor has been neglected since no special task was required of the test pilots during the experiment, besides holding the controls in the desired position.

The second factor has been neglected as well, since the pilots' task did not imply any steady loading of the muscles, besides reacting gravity, so no significant tiring was expected, although muscles' fatigue can incur even after a short time whenever they are required to perform even light tasks.

The overall virtual power results by adding all contributions from the rigid bodies that represent the limbs and from the deformable lumped components that represent the articulations, namely

$$\delta\mathcal{P} = \sum_i \delta\mathcal{P}_{\mathrm{inertia}_i} + \sum_j \delta\mathcal{P}_{\mathrm{articulations}_j}. \tag{25}$$

The optimal value of the constitutive parameters is obtained by defining the functional

$$J = \frac{1}{2T}\int_0^T \delta\mathcal{P}^2 \,\mathrm{d}t, \tag{26}$$

which is minimized according to the least-squares technique, as a function of the lumped deformable components' constitutive parameters.

6 Applications

The transfer functions identified from the experiments discussed earlier in this work have been applied to the realistic light helicopter multibody model described in [10]. The hover flight condition has been addressed, with respect to the vertical bouncing issue.

The first set of analyses have been performed using the pilot's transfer function from [8]; the mesomorphic case of Eq. (1) has been considered, but similar results can be obtained with the transfer function related to the ectomorphic case. The second set of analyses have been performed using the pilot's transfer function of Eq. (3), with data corresponding to Pilot #1 at the 10% collective setting, according to Table 2.

The analysis of the rotorcraft, without any purely mechanical feedback from the pilot's seat motion into the collective control stick, when subjected to a perturbation of the collective control, did not show any significant response of the airframe modes.

With the pilot biomechanical model in the loop, the behavior changes significantly. The pilot appears to significantly couple with the airframe; its specific poles change, and a significant damping reduction is observed. As mentioned earlier, the two transfer functions have been obtained from different types of measurements, and for different cockpit and collective control stick layouts, so a direct comparison is not straightforward. In any case, the comparison of the effects of the two functions on the dynamic behavior of a rotorcraft model provides interesting insight into the problem. In fact, as shown in Figure 11, when the mesomorphic pilot's transfer function is used an instability is found for that root after the pilot's gain is arbitrarily increased. When the transfer function of Eq. (3) is used, both its poles show a significant coupling with the rotorcraft dynamics. However, in this case it is the higher one that finally destabilizes the system when the gain is arbitrarily increased by an appropriate amount. Recall that it is the lower frequency pole of Eq. (3) that corresponds to the pole of Eq. (11).

Note that increasing the gain can sound ar-

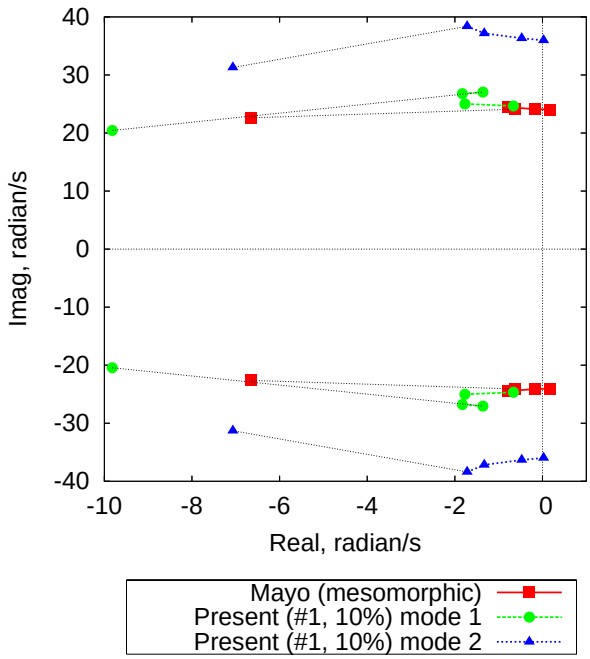

Fig. 11 Coupled rotorcraft-pilot root locus of the pilot's poles.

bitrary, especially for rotorcraft with no FCS but, for example, an increase can be obtained by changing the ratio of the collective pitch change with respect to the collective control stick motion.

7 Concluding Remarks

The work presented in this paper is not concluded yet. The identification of those biomechanical properties of the pilot that would allow an equivalent multibody model to be implemented still requires some tuning. However, very interesting results have already been obtained, and further activity is planned and ongoing. The capability to exploit the experimentally identified biomechanical models within aeroservoelastic rotorcraft simulations is already available, and has already showed that the modeling of the pilot's dynamics can have an impact on the dynamic and aeroelastic properties of the rotorcraft.

References

[1] F. D. Harris, E. D. Kasper, and L. Iseler, "US civil rotorcraft accidents, 1963 through 1997," TM 2000-209597, NASA, 2000.

[2] R. B. Walden, "A retrospective survey of pilot-structural coupling instabilities in naval rotorcraft," in 63rd *Annual Forum of the American Helicopter Society*, (Virginia Beach, VA), May 1–3 2007.

[3] AGARD, "AGARD FVP workshop pilot induced oscillations," AR 335, AGARD, February 1995.

[4] D. T. McRuer, *Aviation Safety and Pilot Control: Understanding and Preventing Unfavorable Pilot-Vehicle Interactions*. Washington D.C.: National Research Council, National Academy Press, 1997.

[5] T. Groot, H. J. Damveld, M. Mulder, and M. M. van Paassen, "Effects of aeroelasticity on the pilot's psychomotor behavior," in *AIAA Atmospheric Flight Mechanics Conference and Exhibit*, (Keystone, Colorado), 21–24 August 2006. AIAA 2006-6494.

[6] G. D. Padfield and M. D. White, "Flight simulation in academia; HELIFLIGHT in its first year of operation," *The Aeronautical Journal of the Royal Aeronautical Society*, vol. 107, pp. 529–538, September 2003.

[7] *FLIGHTLAB Theory Manual (Vol. One)*. Mountain View, California, March 2004.

[8] J. R. Mayo, "The involuntary participation of a human pilot in a helicopter collective contrl loop," in 15th *European Rotorcraft Forum*, (Amsterdam, The Netherlands), pp. 81.1–12, 12–15 September 1989.

[9] T. Parham Jr. and L. M. Corso, "Aeroelastic and aeroservoelastic stability of the BA 609," in *25th European Rotorcraft Forum*, (Rome, Italy), September 14–16 1999.

[10] P. Masarati, G. Quaranta, J. Serafini, and M. Gennaretti, "Numerical investigation of aeroservoelastic rotorcraft-pilot coupling," in *XIX^{o} Congresso Nazionale AIDAA*, (Forlì, Italy), 17–21 Settembre 2007.

[11] P. Eberhard, T. Spägele, and A. Gollhofer, "Investigations for the dynamical analysis of human motion," *Multibody System Dynamics*, vol. 3,

pp. 1–20, 1999.

[12] M. P. T. Silva and J. A. C. Ambrósio, "Kinematic data consistency in the inverse dynamic analysis of biomechanical systems," *Multibody System Dynamics*, vol. 8, pp. 219–239, 2002.

[13] A. Kecskeméthy and A. Weinberg, "An improved elasto-kinematic model of the human forearm for biofidelic medical diagnosis," *Multibody System Dynamics*, vol. 14, pp. 1–21, 2005.

[14] M. Vukobratović, V. Potkonjak, K. Babković, and B. Borovac, "Simulation model of general human and humanoid motion," *Multibody System Dynamics*, vol. 17, pp. 71–96, 2007. doi:10.1007/s11044-006-9034-2.

[15] W. Blajer, K. Dziewiecki, and Z. Mazur, "Multibody modeling of human body for the inverse dynamics analysis of sagittal plane movements," *Multibody System Dynamics*, vol. 18, pp. 217–232, 2007. doi: 10.1007/s11044-007-9090-2.

[16] X. Chenut, P. Fisette, and J.-C. Samin, "Recursive formalism with a minimal dynamic parameterization for the identification and simulation of multibody systems. application to the human body," *Multibody System Dynamics*, vol. 8, pp. 117–140, 2002.

[17] G. Höhne, "Computer aided development of biomechanical pilot models," *Aerospace Science and Technology*, vol. 4, pp. 57–69, January 2000.

[18] "MBDyn - multibody dynamics." http://www.aero.polimi.it/˜mbdyn/.

[19] A. Fumagalli, G. Gaias, and P. Masarati, "A simple approach to kinematic inversion of redundant mechanisms," in *IDETC/CIE 2007 ASME 2007*, (Las Vegas, Nevada, USA), September 4–7 2007. DETC2007-35285.

[20] A. Fumagalli, P. Masarati, and A. Ercoli Finzi, "Feedback dynamic compensation via multibody models and applications to robot control," in *Multibody Dynamics 2007, ECCOMAS Thematic Conference*, (Milano, Italy), June 25–28 2007.

[21] H. Cheng, L. Obergefell, and A. Rizer, "Generator of body (GEBOD) manual," Tech. Rep. AL/CF-TR-1994-0051, Air Force Materiel Command, Wright-Patterson Air Force Base, Ohio, 1994.

Copyright Statement